



<https://jssr.ui.ac.ir/?lang=en>

Journal of Stratigraphy and Sedimentology Researches
E-ISSN: 2423-8007
Vol. 39, Issue 4, No. 93, Winter 2024, pp 1-12
Received: 15.08.2023 Accepted: 01.11.2023

Research Paper

A planktonic foraminiferal record from the Cenomanian/Turonian boundary interval of the Kopet-Dagh Basin (NE Iran)

Behnaz Kalanat *

Department of Palaeobotany, Research Institute of Forests and Rangelands, Agricultural Research, Education and Extension Organization (AREEO),
Tehran, Iran
Kalanat@rifr-ac.ir

Mohamad Hosein Mahmudy Gharai 

Department of Geology, Faculty of Science, Ferdowsi University of Mashhad, Mashhad, Iran
mhmgaraie@um.ac.ir

Abstract

The shale-marlstone interval of the upper Aitamir-lower Abderaz formations in the southeastern part of the Kopet-Dagh Basin was investigated using planktonic foraminiferal studies to determine how surface and water column characteristics of the basin were influenced by Cenomanian/Turonian (C/T) boundary conditions. Three planktonic foraminiferal biozones (upper part of the *Rotalipora cushmani* Total Range Zone, *Whiteinella archaeocretacea* Interval Zone, and lower part of the *Helvetoglobotruncana helvetica* Total Range Zone) have been identified in the studied section, which suggests a late Cenomanian–early Turonian age for this interval. The Aitamir-Abderaz boundary is supposed to be conformable in this section because of the presence of all the C/T boundary planktonic foraminiferal biozones and no evidence of subaerial exposure in the field. The presence of benthic foraminifera throughout the studied section indicates that the anoxic event 2 (OAE2) interval in this succession has never experienced a complete oxygen depletion at the bottom water. However, the low diversity of planktonic foraminifera and low abundance of specialized species indicate more stressful conditions due to intensified weathering and higher productivity (eutrophic conditions) during the OAE2 interval. This interval is punctuated by a transient period with higher diversity of planktonic foraminifera and more abundance of specialized species at the upper part of *R. cushmani* biozone-lower part of *W. archaeocretacea* biozone. This interval can correspond to the “Plenus Cold Event” and demonstrates more stable and oligotrophic conditions across the OAE2.

Keywords: Palaeoecology, OAE2, Planktonic foraminifera, Biostratigraphy

Introduction

The oceanic anoxic event 2 (OAE2; Schlanger et al. 1987) is the most significant OAE in the Cretaceous, which has caused extensive palaeontologic, palaeoceanographic and sedimentologic consequences during the Cenomanian/Turonian (C/T) boundary interval (e.g., Kuypers et al. 2002; Kolonic et al. 2005). This event occurs during the warmest interval of the Cretaceous greenhouse and is characterized by surface and bottom water temperatures far higher than today (Bornemann et al. 2008; Friedrich et al. 2008). These conditions accelerated hydrological cycles and caused a fundamental change in marine productivity and eutrophication (Jenkyns 2010). The widespread deposition of black shale at this time went along with oxygen deficiency in deep waters as well as the photic zone (e.g., Kuhnt et al. 1990; Kuypers et al. 2002; Pancost et al. 2004).

This environmental perturbation was associated with significant extinction events and faunal turnovers (e.g., Erbacher and Thurow 1997; Premoli Silva et al. 1999; Leckie et al. 2002). Among the planktonic foraminifera, rotaliporids disappeared at the onset of this event. Other assemblages of planktonic foraminifera were generally poorly diversified and dominated by small-sized stress markers, indicative of meso-eutrophic conditions and/or expansion of oxygen minimum zone (Leckie et al. 1998, 2002; Coccioni and Luciani 2004, 2005; Elderbak et al. 2014; Reolid et al. 2015; Kalanat et al. 2016; Falzoni et al. 2016; Kalanat and Vaziri-Moghaddam 2019b).

The geochemical and palaeontological studies in several sections in the northeast of the Kopet-Dagh Basin indicate a gradual perturbation of the environment during the C/T boundary (Kalanat et al. 2016, 2017, 2018a, b; Gharai and Kalanat 2018). These studies revealed that the real black shale (with

*Corresponding author

Kalanat, B., and Mahmudy Gharai, M. H. (2024). A planktonic foraminiferal record from the Cenomanian/Turonian boundary interval of the Kopet-Dagh Basin (NE Iran). *Journal of Stratigraphy and Sedimentology Researches*, 39(4): 1-12. doi: [10.22108/jssr.2023.138780.1265](https://doi.org/10.22108/jssr.2023.138780.1265)



2423-8007 / © 2023 University of Isfahan

This is an open access article under the CC BY-NC-ND 4.0 License (<https://creativecommons.org/licenses/by-nc-nd/4.0/>).



<https://doi.org/10.22108/jssr.2023.138780.1265>

total organic carbon (TOC) > 1%) was not deposited in the NE of the Kopet-Dagh basin but the warm-wet periods are characterized by higher $p\text{CO}_2$ and TOC values (Kalanat et al. 2018a, b), higher detrital input (Gharaie and Kalanat 2018), and near absence of planktonic foraminifera (Kalanat et al. 2016). These conditions suggest that this interval in the Kopet-Dagh Basin was influenced by wet-dry periods and fresh water influx into the basin (Kalanat et al. 2017).

Here, we aim to study planktonic foraminifera across the C/T boundary to reconstruct the palaeoenvironmental conditions of the OAE2 in the surface and water column of the Shurab section in the southeast of Kopet-Dagh Basin (north of Tethys Ocean).

Geological setting and study area

Opening and closure of the Paleotethys and Neotethys oceans have played fundamental roles in the geological history of Iran (Robert et al. 2014). The opening of Neotethys started from Late Carboniferous to late Early Permian, which resulted in detachment of Cimmerian blocks from the northern margin of the Gondwana and increasing slab-pull forces in Paleotethys (Stampfli and Borel 2002; Muttoni et al. 2009). This was followed by the subduction of Paleotethys's mid-ocean ridge below the Eurasian margin and the final closure of Paleotethys in the middle Triassic time (Stampfli and Borel 2002). The Kopet-Dagh was one of the Permo-Triassic marginal basins, which formed after the Cimmerian collision and the opening of

back-arc oceans in the north of Iran. This basin was developed from the Jurassic to Neogene along the southern margin of Eurasia (Stampfli and Borel 2002; Robert et al. 2014) (Fig. 1A). During this time about 7–12 km of predominantly marine strata deposited in the basin without major sedimentary breaks (Afshar-Harb 1994). The Albian–Cenomanian succession of the Kopet-Dagh Basin is characterized by the siliciclastic deposits (shale and sandstone) of the Aitamir Formation. By the end of Cenomanian a worldwide sea level rise was accompanied by deposition of a green shale unit at the top of the Aitamir Formation in the east of the basin (Kalanat et al. 2018a). Overlying this Formation, the offshore-marine deposits of the Turonian–Campanian Abderaz Formation are mostly made up of calcareous marl and chalky limestone (Afshar-Harb 1994).

The studied section is well exposed in the southeast of the Kopet-Dagh Basin at the Shurab Anticline. It is located 80 km to the southeast of Mashhad city, near the Shurab village (35°56'16"N, 60°36'34"E) (Fig. 1B, C). The stratigraphic interval spans the upper part of Aitamir and lower part of the Abderaz formations. It is predominantly composed of 40 m-thick shales and marlstones. The lithology shows a gradual change from olive green shales to white color marlstones towards the top of the section (Fig. 1D). No evidence of unconformity was observed between the Aitamir-Abderaz formations in the field.

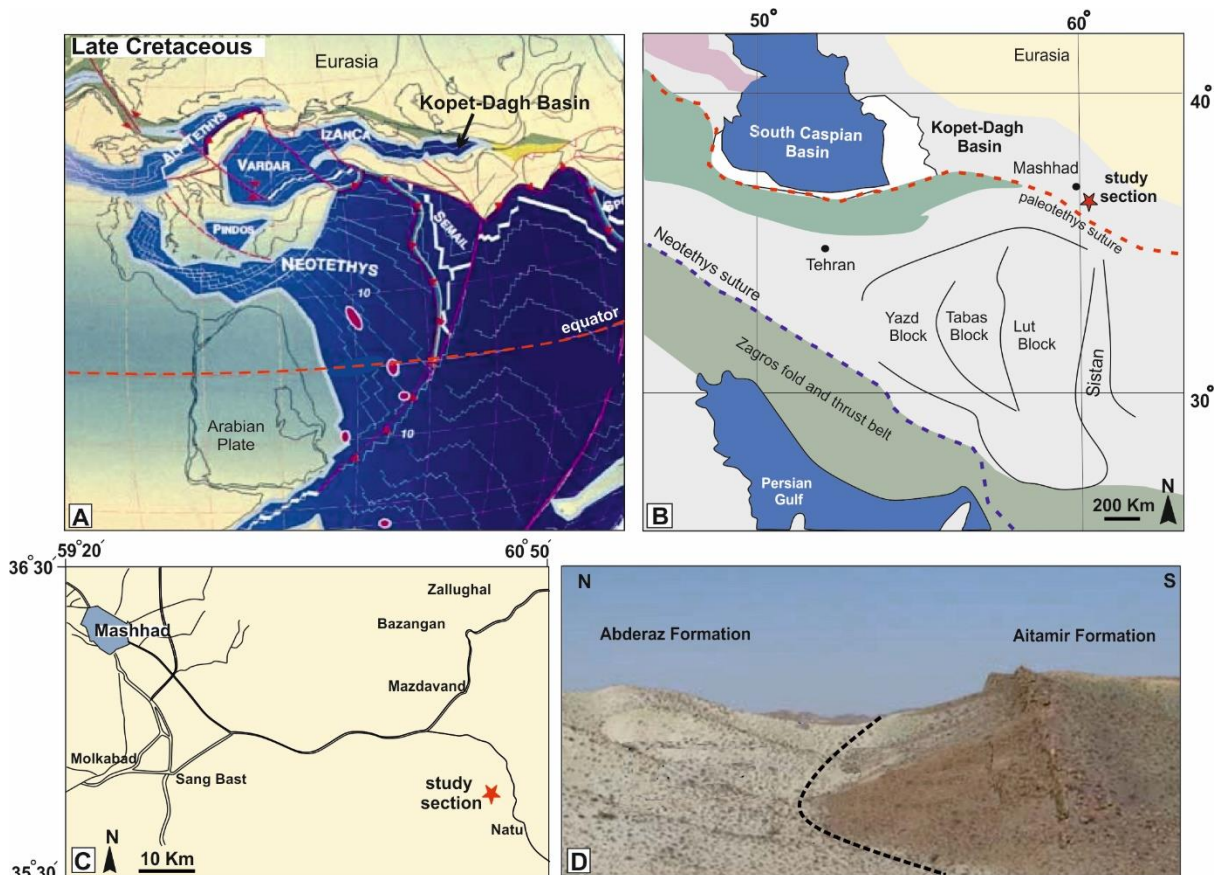


Fig 1- A- Late Cretaceous (160 Ma) palaeogeographic map of the Middle East; the Kopet-Dagh Basin is indicated along the Eurasian margin (Stampfli and Borel 2002). B, C- Location map of studied section (Shurab) in the southeast of Mashhad city, northeast of Iran. The location of the Paleotethys and Neotethys suture zones and Kopet-Dagh Basin are indicated in Figure B (modified after Angiolini et al. 2007). D- Field photograph of the Aitamir-Abderaz boundary in the Shurab section.

Material & Methods

Following the preliminary sampling to determine the position of the C/T boundary, 28 representative samples were collected over a 40 m-thick section. Samples were taken over 1–2 m at the base and top of the outcrop, but the sample spacing was more detailed (0.5 m) close to the C/T boundary. For the study of the foraminiferal population, samples were crushed to pea-size pieces and soaked in a 5% hydrogen peroxide solution for at least 24 h. The samples were then washed over 63, and 125 µm sieves and analyzed for planktonic foraminifera based on the count of 200–300 specimens. The ratio of planktonic to benthic foraminifera, simple diversity (number of species) and Shannon-Wiener diversity index (H(s); Murray 1991) were also determined in the study section.

Taxonomic concepts for planktonic foraminiferal species applied in this study follow the description and classification of Mesozoic planktonic foraminifera in the online dictionary located at <http://www.mikrotax.org>.

Results

Planktonic foraminifera

Twelve genera and thirty species of planktonic foraminifera

are recognized in the study section (Figs. 2, 3, 4 and Supplementary Table 1). Planktonic foraminifera dominate the foraminiferal assemblages throughout the section (60–85%) except for the lower part of succession (AS42–AS62), where the benthic foraminifera are more abundant. The species richness and H(s) of planktonic foraminifera fluctuate from 7 to 18 and from 1.1 to 2.1, respectively.

Whiteinella is the most abundant genus in the studied interval, however, its proportion decreases at the top of the section, where an abundance of the biserial morphotype (*Planoheterohelix*) gradually increases to more than 40% (AS109–AS129). Keelid planktonic foraminifera including *Rotalipora*, *Thalmaninella*, *Dicarinella* and *Praeglobotruncana* as well as planispiral morphotype ("*Globigerinelloides*") are rare throughout the section (<10%), but they become more abundant at AS78–AS88, where diversity of planktonic foraminifera reaches a maximum (H(s) up to two and species richness up to 18). Triserial assemblage (*Guembelitra*) are more abundant in the lower part of the studied interval (about 10%) but they become rare or even absent at the top of the section (AS78–AS139) (Fig. 2).

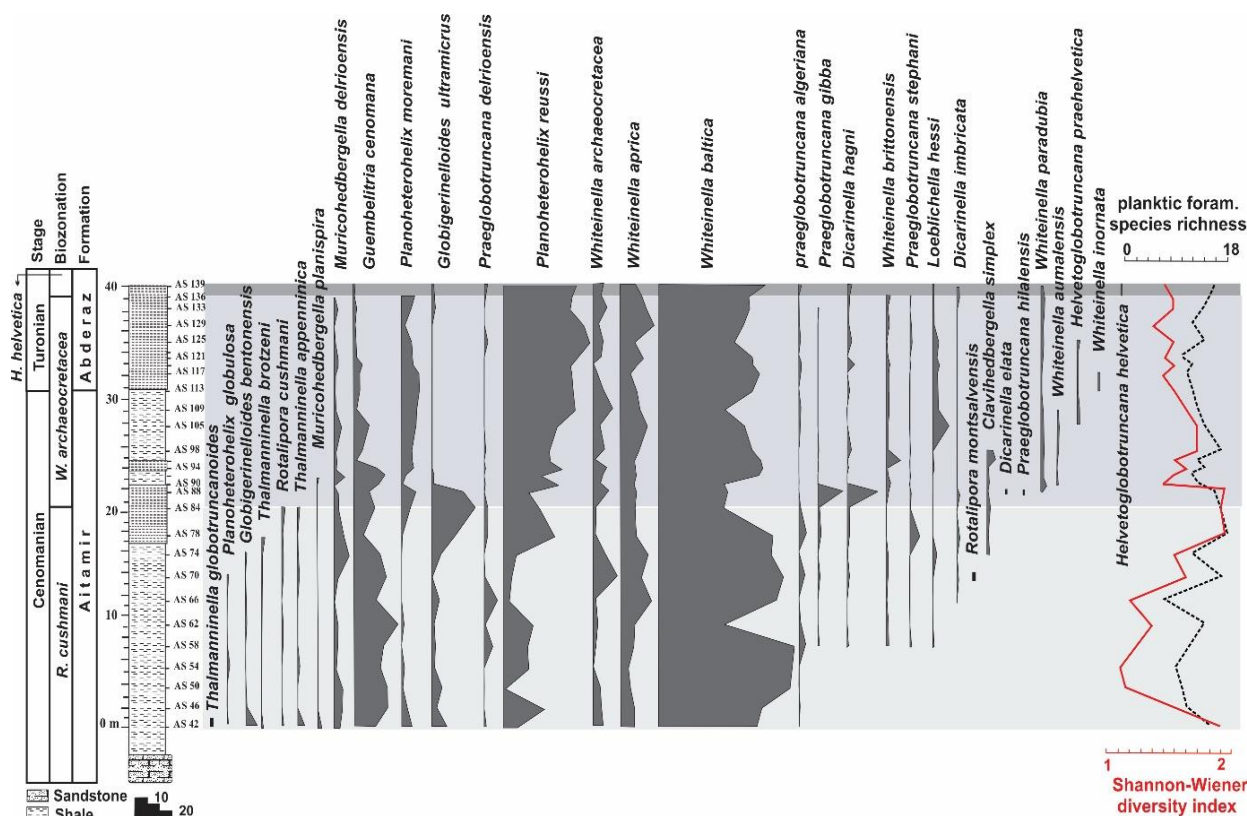


Fig 2- Stratigraphic distribution and abundance of planktonic foraminiferal species in the Shurab section. Species richness and Shannon-Wiener diversity index are also plotted.

Biostratigraphy

Based on the established zonal scheme of Robaszynski and Caron (1995) for low to mid-latitude planktonic foraminifera, which has been used and revised in several works (e.g., Keller et al. 2001; Premoli-Silva and Verga 2004; Caron et al. 2006; Coccioni and Premoli Silva 2015; Elderbak and Leckie 2016; Falzoni et al. 2016, 2018; Kalanat and Vaziri-Moghaddam 2019b; Falzoni and Petrizzo 2020), three following biozones were identified in the Shurab section:

Rotalipora cushmani Biozone (late middlelatest Cenomanian; AS42–AS88; Aitamir Formation): this biozone is defined as the total range of nominate taxon by Premoli-Silva and Verga (2004). Coccioni and Premoli-Silva (2015) have defined this biozone as the interval from the highest occurrence (HO) of *Thalmaninella reicheli* to HO of *R. cushmani*. This biozone is subdivided into two subzones. *Thalmaninella greenhornensis* (late middle to early late Cenomanian) subzone is defined as the interval from HO of *Thalmaninella reicheli* to the lowest occurrence (LO) of *Praeglobotruncana algeriana*. *P. algeriana* (formerly known as *Dicarinella algeriana*) subzone (early late to latest Cenomanian) is the interval from the LO of the zonal marker to the HO of *Rotalipora cushmani*.

The presence of *P. algeriana* from the base of the Shurab section indicates that the lower part of this succession spans the *P. algeriana* subzone and is assigned to the late Cenomanian. This subzone continues to the extinction of *R. cushmani* at 22 m. Whitinellids and heterohelicids are the main components of this interval. Rotaliporids, globigerinelloids, muricohedbergellids, guembelitrids, dicarinellids, praeglobotruncanids and Thalmaninnellids are also present.

Whiteinella archaeocretacea Partial Range Zone (latest Cenomanian–earliest Turonian; AS90–AS133; the upper part of the Aitamir–lower part of the Abderaz formations) spans the interval from the HO of *R. cushmani* to the LO of *Helvetoglobotruncana helvetica*. The foraminiferal assemblages in this biozone are dominated by heterohelicids, whiteinellids and muricohedbergellids. The C/T boundary is placed toward the top of this interval but the position of the boundary cannot be defined precisely by planktonic foraminifera.

Helvetoglobotruncana helvetica Total Range Zone (early Turonian; AS136–AS139; Abderaz Formation) is characterized by the total range of the zonal marker. The lower part of this biozone was determined in the upper two meters of the studied section. The foraminiferal assemblage in this interval is dominated by heterohelicids, whiteinellids and muricohedbergellids. *Dicarinella*, *Guembelitra* and *Praeglobotruncana* are less common.

Discussion

Ecological concepts of planktonic foraminifera

Ecological response of different planktonic foraminiferal morpho-groups to palaeoceanographic variations such as depth, nutrient supply, temperature, and stratification of

water column leads to significant changes in these taxa during the C–T interval. While different ecological niches of modern species are relatively well understood (e.g., Hemleben et al. 1989; Spero et al. 1997; Zanic et al. 2005; Kimoto et al. 2009), the palaeoecology of extinct C/T planktonic foraminifera can be inferred from comparison of their morphology with equivalent modern morpho-groups (e.g., Hart and Bailey 1979; Leckie et al. 1998; West et al. 1998; Hart 1999) and from their tests carbon-oxygen isotope signatures (e.g., D'Hondt and Arthur 1995; Huber et al. 1995; Bornemann and Norris 2007; Coxall et al. 2007; Wendler et al. 2013).

The isotope data for heterohelicids are still under debate (e.g., Huber et al. 1995, 1999; Fassell and Bralower 1999; MacLeod et al. 2000; Wendler et al. 2013), but this small-sized simple biserial group is generally considered to occupy a near-surface habitat in high eutrophic conditions (Hart 1999). During the Late Cretaceous heterohelicids dominated the low-oxygen marine environments (Hart and Ball 1986; Leckie et al. 1998). Therefore, their dominance can be a good indicator of well-developed oxygen minimum zones.

Triserial species (*Guembelitra*) is known to thrive under unstable shallow marine environments with variations in salinity, temperature and nutrients (Leckie et al. 1998; Keller 2002; Keller et al. 2002, 2008; Keller and Pardo 2004a).

The small-sized planispiral taxon, "*Globigerinelloides*", is typically inferred to reflect an environment below the surface mixed layer, but above keeled morphotypes (Keller et al. 2002; Leckie et al. 2002; Coccioni and Luciani 2004). They tolerated less variable conditions compared to eutrophic and opportunist groups like hedbergellids and heterohelicids, and thrived in mesotrophic conditions (Hart 1999; Premoli Silva and Sliter 1999; Friedrich et al. 2003; Friedrich et al. 2018).

Stable isotope data suggested that whitinellids occupied the lower part of the mixed layer (Norris and Wilson 1998). Coccioni and Luciani (2004) suggested that their high reproduction potential (high abundance) indicates that these taxa tolerated the eutrophic conditions.

Hedbergellids are opportunistic taxa, thriving in both open marine and epicontinental settings in different latitudes (e.g., Premoli Silva and Sliter 1999). The isotopic data from the C/T boundary indicated that this group inhabited surface or near-surface waters (Corfield et al. 1990; Price and Hart 2002). They were adapted to eutrophic environments (Hart 1999; Keller et al. 2001) and a wide range of temperature-related habitats (Price et al. 1998).

Stable isotope ranking indicated that among keeled groups in the C/T boundary, large and complex rotaliporids and thalmaninellids are the most specialized species, which occupied deeper oligotrophic waters at or below thermocline depth (e.g., Corfield et al. 1990; Price and Hart 2002; Norris and Wilson 1998; Keller et al. 2001; Keller and Pardo 2004b; Coccioni and Luciani 2004). *Dicarinella* and *Praeglobotruncana* are medium-sized weekly-keeled genera, which are considered as an intermediate dwellers and intermediate strategists (Premoli Silva and Sliter 1999; Keller et al. 2001; Keller and Pardo 2004b; Coccioni and Luciani 2004).



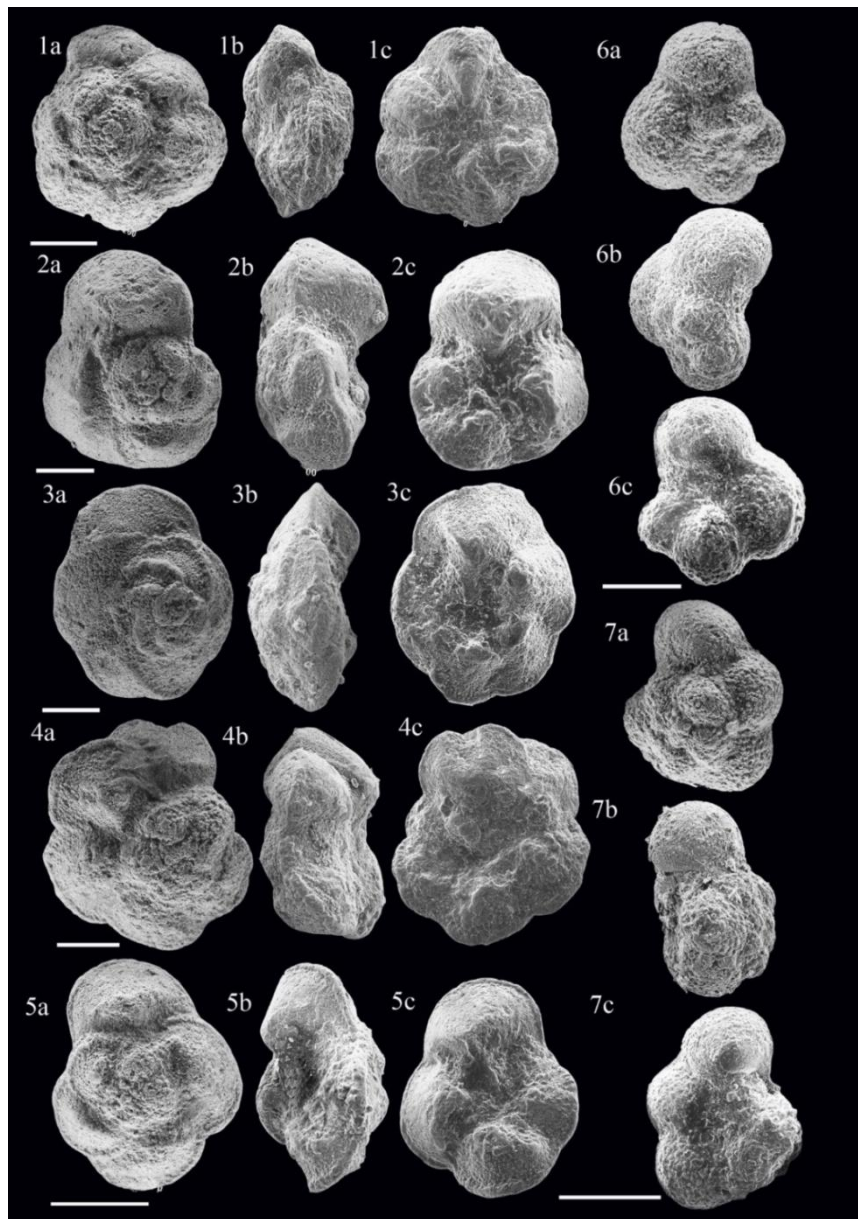


Fig 3- 1. *Rotalipora cushmani* (Morrow), sample 70 (scale bar= 200 μm). 2. *Rotalipora cushmani* (Morrow), sample 60 (scale bar = 100 μm). 3. *Thalmanninella globotruncanoides* (Sigal), sample 42 (scale bar = 100 μm). 4. *Thalmanninella brotzeni* (Sigal), sample 42 (scale bar = 100 μm). 5. *Thalmanninella appenninica* (Renz), sample 60 (scale bar = 100 μm). 6. *Whiteinella baltica* Douglas and Rankin, sample 42 (scale bar = 100 μm). 7. *Whiteinella paradubia* (sigal), sample 72 (scale bar = 100 μm).

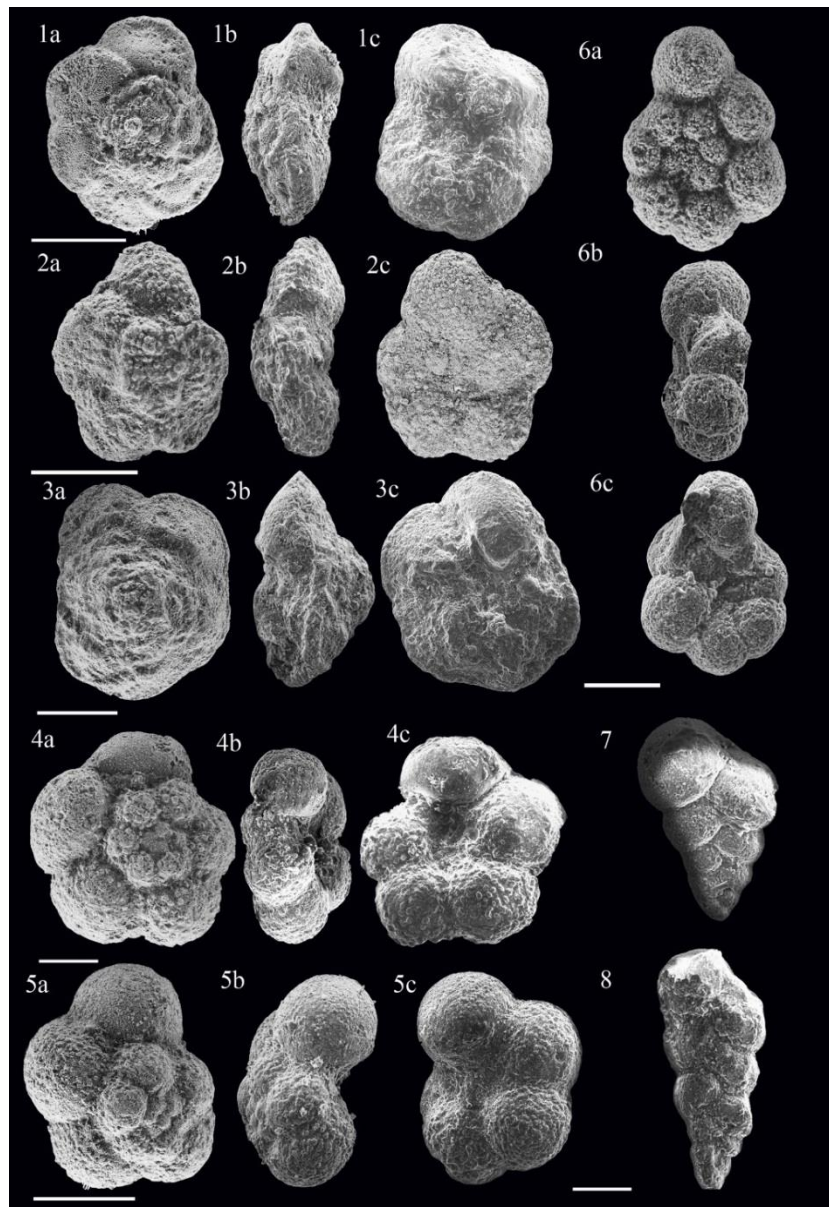


Fig 4- 1. *Dicarinella hagni* (Scheibnerova), sample 70 (scale bar = 200 μm), 2. *Praeglobotruncana algeriana* (Caron), sample 42 (scale bar = 200 μm). 3. *Praeglobotruncana hilalensis* Barr, sample (scale bar = 100 μm). 4. *Whiteinella archaeocretacea* Pessango, sample 74 (scale bar = 100 μm). 5. *Whiteinella brittonensis* (Loeblich and Tappan), sample 74 (scale bar = 100 μm). 6. *Muricohedbergella planispira* (Tappan), sample 42 (scale bar = 50 μm). 7. *Planoheterohelix reussi* (Cushman), sample 88 (scale bar = 50 μm). 8. *Planoheterohelix moremani* (Cushman), sample 88 (scale bar = 50 μm).

OAE2 interval in the Shurab section

The global and regional changes in the environmental conditions during the OAE2 interval are correlated with the variations in the planktonic foraminiferal assemblages and diversity in the Shurab section. Based on these changes, the C/T boundary succession (OAE2) in the Shurab section can be divided into three intervals (Fig. 5).

Interval 1 (A46–A74; upper part of *R. chushmani* Biozone): the initiation of OAE2 is generally characterized

by magmatic activities, which are introduced by large concentrations of trace metals (caused by high hydrothermal activities) at the same time turnover in plankton communities, and increases in isotopically light organic carbon burial occurred (Arthur et al. 1985; Larson 1991; Snow et al. 2005; Seton et al. 2009). High atmospheric $p\text{CO}_2$ (warm conditions) (e.g., Fletcher et al. 2008; Barclay et al. 2010), higher hydrological cycles, and continental weathering (eutrophication) (Pogge von Strandmann et al. 2013) are other characteristics of this



interval. The evidence of higher $p\text{CO}_2$ (Ghahesu and Taherabad sections; Kalanat et al. 2018a, b) and silicate weathering (Hamam-Ghaleh section; Gharai and Kalanat 2018) has been documented in the Kopet-Dagh Basin. The chemical weathering is documented by an increase in kaolinite/illite ratios in this interval (the upper part of the Aitamir Formation).

The dark shales of the Aitamir Formation at the lower part of the Shurab section is characterized by low diversity planktonic foraminifera and higher benthic/planktonic ratios. This is accompanied by the presence of *Guembelitra* and a high abundance of trochospiral morpho-groups (*Whiteinella*), which suggest relatively shallow water eutrophic conditions. This interval can be correlated with the warm-eutrophic period at the beginning of the OAE2 interval.

Interval 2 (A78–A88, uppermost part of *R. chushmani* Biozone and lower part of *W. archaeocretacea* Biozone): The widespread carbon burial and silicate weathering are the effective factors in drawdown atmospheric $p\text{CO}_2$ and reducing the temperature (Arthur et al. 1988; Freeman and Hayes 1992; Kuypers et al. 1999; Pogge von Strandmann et al. 2013), causing a cold event in the subsequent interval of OAE2, which is characterized by higher oxygen isotope values and lower $p\text{CO}_2$ ($\delta^{13}\text{C}_{\text{carb}} - \delta^{13}\text{C}_{\text{org}}$). This interval (namely “Plenus Cold Event” in Europe; Jefferies 1962; Gale and Christensen 1996; Voigt et al. 2004; Jarvis et al. 2011; Jenkyns et al. 2017 and “Benthonic zone” in Western Interior Seaway of North America; Leckie et al. 1998; Elderbak et al. 2014; Elderbak and Leckie 2016) is closely related to a sea level transgression (according to aquifer eustasy hypothesis; see Wendler et al. 2011, 2016a, b; Kalanat et al. 2018a; Kalanat and Vaziri-Moghaddam 2019a). In the Kopet-Dagh Basin, it is characterized by reduced $p\text{CO}_2$ and lower values of detrital input (Kalanat et al. 2018a, b; Gharai and Kalanat 2018), suggesting colder and drier conditions.

The Shurab section represents a dramatic increase in the diversity of planktonic foraminifera and a higher abundance of keeled and planispiral morphotypes in this interval. These conditions associated with Lower benthic/plankton ratios and a decrease of *Guembelitra* abundance as a marginal marine taxa (e.g., Keller 2002) suggest higher sea level and more stable oligotrophic conditions at the surface water.

The HO of *Rotalipora* occurs at the middle part of this interval. This is corresponded to other records in the Kopet-Dagh Basin (Kalanat et al. 2018a, b), northern Europe (Pearce et al. 2009), Spanish sections (Kaiho et al. 2014), Western Interior Seaway (Elderbak and Leckie 2016), and Morocco (Kuhnt et al. 2017). The relationship between cooling and extinction of *Rotalipora* has been attributed to the disruption of thermal stratification of the water column, the effect of cooling on this thermophilic foraminifera, and also the loss of the principal food source of *Rotalipora* during the cooling event (Falzoni and Petrizzo 2020).

Interval 3 (A90–A129; upper part of the *W. archaeocretacea* Biozone): After a transient cooling, the renewed CO_2 outgassing (Turgeon and Creaser 2008) resulted in almost similar conditions (warm-wet) to the start of OAE2 interval. This is associated with a major flux of fresh water to the Kopet-Dagh Basin, causing a negative oxygen isotope shift, increased kaolinite contents, and detrital input (Kalanat et al. 2018a).

In the Shurab section, these conditions coincide with the decrease in diversity, low abundance of specialized planktonic foraminifera, and high numbers of *Planoheterohelix*, which indicate a eutrophic environment and expansion of oxygen minimum zone. An abrupt increase in abundance of *Planoheterohelix* (“*Heterohelix*” shift; Leckie et al. 1998) is also documented in low latitude records across the OAE2 such as Eastbourne, England (Keller et al. 2001), Tarfaya, Morocco (Falzoni et al. 2018), Umbria-Marche Basin, Italy (Coccioni and Luciani 2004, 2005), Western Interior Seaway Pueblo, Colorado (Leckie et al. 1998; Elderbak and Leckie 2016); and Zagros Basin, Iran (Kalanat and Vaziri-Moghaddam 2019b).

The relative decrease of biserial planktonic foraminifera and the appearance of a new specialized species (*H. helvetica*) can be interpreted as gradual re-establishment of stable conditions at the uppermost part of the section.

Conclusion

The Shurab section at the SE of Kopet-Dagh Basin (NE Tethyan realm) spans the OAE2 interval during the C/T boundary. The variations in the diversity and morphotypes of the planktonic foraminifera led us to subdivide the OAE2 succession into three intervals. The first and third intervals are characterized by a low diversity of planktonic foraminifera and a higher abundance of opportunistic surface dweller taxa (e.g., hedbergellids and heterohelicids). This suggests high productivity conditions at the surface water of the basin, which most likely was caused by higher weathering and detrital input during the warm and humid periods. The second interval represents a short-lived planktonic foraminiferal repopulation, indicating more oligotrophic conditions at the upper part of *R. chushmani* Biozone-lower part of *W. archaeocretacea* Biozone (corresponding to “Plenus Cold Event”).

The turnover of planktonic foraminifera in the studied section is characterized by the extinction of rotaliporids and “*Heterohelix*” shift. The last occurrence of rotaliporids falls within the “Plenus Cold Event”, which suggests that the extinction of these warm-water taxa may have been caused by the cooling of the water column. Heterohelicid dominance occurs in the third interval of OAE2 at the upper part of *W. archaeocretacea* Biozone, demonstrating eutrophication and expansion of the oxygen minimum zone to the surface water.



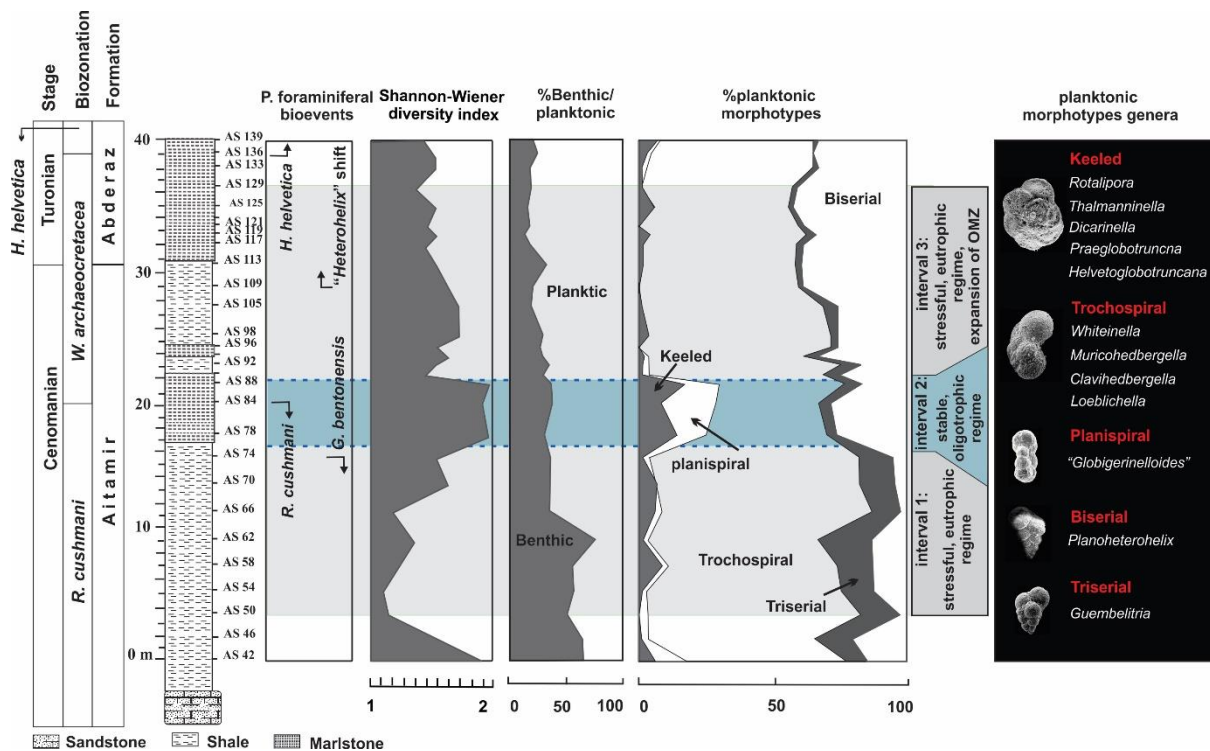


Fig 5- Planktonic foraminiferal variations and environmental perturbation during the C/T boundary interval in the Shurab section (Kopet-Dagh Basin).

Acknowledgments

The authors sincerely acknowledge Prof. H. Vaziri-Moghaddam for the editorial management of the manuscript and Dr. M.A. Salehi for improving the English text. We are also grateful to two anonymous reviewers, whose constructive comments helped us to improve the quality of this manuscript.

References

- Afshar-Harb A. 1994. The geology of the Koppah Dagh, Iran. Geological survey of Iran, Tehran, 275 p.
- Angiolini L. Gaetani M. Muttoni G. Stephanson M.H. and Zanchi A. 2007. Tethyan oceanic currents and climate gradients 300 m.y. ago. *Geology*, 35: 1071–1074. <https://doi.org/10.1130/G24031A.1>
- Arthur M.A. Dean W.E. and Pratt L.M. 1988. Geochemical and climatic effects of increased marine organic carbon burial at the Cenomanian/Turonian boundary. *Nature*, 335: 714–717.
- Arthur M.A. Dean W.E. and Schlanger S.O. 1985. Variations in the global carbon cycle during the Cretaceous related to climate, volcanism, and changes in atmospheric CO₂. In: Sundquist E.T. and Broecker W.S. (Eds.), *The Carbon Cycle and Atmospheric CO₂: Natural Variations Archean to Present*. American Geophysical Union Geophysical Monograph Series, 32: 504–529.
- Barclay R.S. McElwain J.C. and Sageman B.B. 2010. Carbon sequestration activated by a volcanic CO₂ pulse during Ocean Anoxic Event 2. *Nature Geoscience*, 3: 205–208.
- Bornemann A. and Norris R.D. 2007. Size-related stable isotope changes in Late Cretaceous planktonic foraminifera: Implications for paleoecology and photosymbiosis. *Marine Micropaleontology*, 65: 32–42. <https://doi.org/10.1016/j.marmicro.2007.05.005>
- Bornemann A. Norris R.D. Friedrich O. Beckmann B. Schouten S. Sinninghe Damsté J.S. Vogel J. Hofmann P. and Wagner T. 2008. Isotopic evidence for glaciation during the Cretaceous super-greenhouse. *Science*, 319: 189–192. doi: 10.1126/science.1148777
- Caron M. Dall'Agnolo S. Accarie H. Barrera E. Kauffman E.G. Amedro F. and Robaszynski F. 2006. High-resolution stratigraphy of the Cenomanian-Turonian boundary interval at Pueblo (USA) and wadi Bahloul (Tunisia): stable isotope and bio-events correlation. *Geobios*, 39: 171–200. <https://doi.org/10.1016/j.geobios.2004.11.004>
- Coccioni R. and Luciani V. 2004. Planktonic foraminifers and environmental changes across the Bonarelli Event (OAE2, latest Cenomanian) in its type area: a high-resolution study from the Tethyan reference Bottaccione section (Gubbio, Central Italy). *Journal of Foraminiferal Research*, 34: 109–129. <https://doi.org/10.2113/0340109>
- Coccioni R. and Luciani V. 2005. Planktonic foraminifers across the Bonarelli Event (OAE2, latest Cenomanian): The Italian record. *Palaeogeography, Palaeoclimatology, Palaeoecology*, 224: 167–185. <https://doi.org/10.1016/j.palaeo.2005.03.039>
- Coccioni R. and Premoli-Silva I. 2015. Revised Upper Albian-Maastrichtian planktonic foraminiferal biostratigraphy and magnetostratigraphy of the classical Tethyan Gubbio section (Italy). *Newsletter on Stratigraphy*, 48: 47–90.
- Corfield R.M. Hall M.A. and Brasier M.D. 1990. Stable isotope evidence for foraminifera habitats during the development of the Cenomanian – Turonian oceanic anoxic event. *Geology*, 18: 175–178.
- Coxall H.K. Wilson P.A. Pearson P.N. and Sexton P.F. 2007.



- Iterative evolution of digitate planktonic foraminifera. *Paleobiology*, 33: 495–516.
- D'Hondt S. and Arthur M.A. 1995. Interspecies variation in stable isotopic signals of Maastrichtian planktonic foraminifera. *Paleoceanography*, 10: 123–135.
- Elderbak K. and Leckie R.M. 2016. Paleocirculation and foraminiferal assemblages of the Cenomanian-Turonian Bridge Creek Limestone bedding couplets: productivity vs. dilution during OAE2. *Cretaceous Research*, 60: 52–77.
- Elderbak K. Leckie R.M. and Tibert N.E. 2014. Paleoenvironmental and paleoceanographic changes across the Cenomanian-Turonian Boundary Event (Oceanic Anoxic Event 2) as indicated by foraminiferal assemblages from the eastern margin of the Cretaceous Western Interior Sea. *Palaeogeography, Palaeoclimatology, Palaeoecology*, 413: 29–48.
- Erbacher J. and Thurrow J. 1997. Influence of oceanic anoxic events on the evolution of mid-Cretaceous radiolaria in the North Atlantic and western Tethys. *Marine Micropaleontology*, 30: 139–158.
- Falzone F. and Petrizzo M.R. 2020. Patterns of planktonic foraminiferal extinctions and eclipses during Oceanic Anoxic Event 2 at Eastbourne (SE England) and other mid-low latitude locations. *Cretaceous Research*, 116: 104593.
- Falzone F. Petrizzo M.R. Caron M. Leckie R.M. and Elderbak K. 2018. Age and syn-chronicity of planktonic foraminiferal bioevents across the Cenomanian-Turonian boundary interval (Late Cretaceous). *Newsletter on Stratigraphy*, 51 (3): 343–380.
- Falzone F. Petrizzo M.R. Jenkyns H.C. Gale A.S. and Tsikos H. 2016. Planktonic foraminiferal biostratigraphy and assemblage composition across the Cenomanian-Turonian boundary interval at Clot Chevalier (Vocontian Basin, SE France). *Cretaceous Research*, 59: 69–97.
- Fassell M.L. and Bralower T.J. 1999. Warm, equable mid-Cretaceous: stable isotope evidence. *GSA Special Publication*, 332: 121–142.
- Fletcher B.J. Brentnall S.J. Anderson C.W. Berner R.A. and Beerling D.J. 2008. Atmospheric carbon dioxide linked with Mesozoic and early Cenozoic climate change. *Nature Geoscience*, 1: 43–48.
- Freeman K.H. and Hayes J.M. 1992. Fractionation of carbon isotopes by phytoplankton and estimates of ancient CO₂ levels. *Global Biogeochemistry Cycles*, 6: 185–198.
- Friedrich O. Bornemann A. Norris R.D. Erbacher J. and Fiebig J. 2018. Changes in tropical Atlantic surface-water environments inferred from late Albian planktonic foraminiferal assemblages (ODP Site 1258, Demerara Rise). *Cretaceous Research*, 87: 74–83.
- Friedrich O. Erbacher J. Moriya K. Wilson P.A. and Kuhnert H. 2008. Warm saline intermediate waters in the Cretaceous tropical Atlantic Ocean. *Nature Geoscience*, 1: 453–457.
- Friedrich O. Reichelt K. Herrle J.O. Lehmann J. Pross J. and Hemleben C. 2003. Formation of the Late Aptian Niveau Falot black shales in the Vocontian Basin (SE France): evidence from foraminifera, palynomorphs, and stable isotopes. *Marine Micropaleontology*, 49: 65–85.
- Gale A.S. and Christensen W.G. 1996. Occurrence of the belemnite *Actinocamax plenus* in the Cenomanian of SE France and its significance. *Bulletin of the Geological Society of Denmark*, 43: 68–77.
- Gharai M.H.M. and Kalanat B. 2018. Enhanced chemical weathering and organic carbon burial as recovery factors for the OAE2 environmental conditions: a case study from Koppeh-Dagh Basin, NE Iran. *Geopersia*, 8: 233–244.
- Hart M.B. 1999. The evolution and biodiversity of Cretaceous planktonic foraminifera. *Geobios*, 32: 247–255.
- Hart M.B. and Bailey H.W. 1979. The distribution of planktonic Foraminiferida in the Mid-Cretaceous of NW Europe; Aspekte der Kreide Europas. *International Union of Geological Sciences*, 6: 527–542.
- Hart M.B. and Ball K.C. 1986. Late Cretaceous anoxic events, sea level changes and the evolution of the planktonic foraminifera. In: Summerhayes, C.P. and Shackleton N.J. (Eds.), *North Atlantic Paleooceanography* Geological Society of America, Special Publications, vol. 21. Geo. Soc. America, Boulder Co, 67–78.
- Hemleben C. Spindler M. and Anderson O.R. 1989. *Modern Planktonic Foraminifera*. Springer, New York, 363 p.
- Huber B.T. Hodell D.A. and Hamilton C.P. 1995. Middle-Late Cretaceous climate of the southern high latitudes: Stable isotopic evidence for minimal equator-to-pole thermal gradients. *Geological Society of America Bulletin*, 107: 1164–1191.
- Huber B.T. Leckie R.M. Norris R.D. Bralower T.J. and CoBabe E. 1999. Foraminiferal assemblage and stable isotopic change across the Cenomanian-Turonian boundary in the subtropical North Atlantic. *Journal of Foraminiferal Research*, 29: 392–417.
- Jarvis I. Lignum J.S. Gröcke D.R. Jenkyns H.C. and Pearce M.A. 2011. Black shale deposition, atmospheric CO₂ drawdown and cooling during the Cenomanian-Turonian Oceanic Anoxic Event. *Paleoceanography*, 26: PA3201.
- Jefferies R.P.S. 1962. The palaeoecology of the *Actinocamax plenus* sub zone (lowest Turonian) in the Anglo-Paris Basin. *Palaeontology*, 4: 609–647.
- Jenkyns H.C. 2010. Geochemistry of oceanic anoxic events. *Geochemistry, Geophysics, Geosystems*, 11: Q03004.
- Jenkyns H.C. Dickson A.J. Ruhl M. and van den Boorn S.H.J.M. 2017. Basalt-seawater interaction, the Plenus Cold Event, enhanced weathering and geochemical change: deconstructing Oceanic Anoxic Event 2 (Cenomanian-Turonian, Late Cretaceous). *Geology*, 64: 16–43.
- Kaiho K. Katabuchi M. Oba M. and Lamolda M. 2014. Repeated anoxia-extinction episodes progressing from slope to shelf during the latest Cenomanian. *Gondwana Research*, 25: 1357–1368.
- Kalanat B. Mahmudy Gharai M.H. Vahidinia M. and Matsumoto R. 2018a. Short-term eustatic sea-level changes during the Cenomanian-Turonian Supergreenhouse interval in the Kopet-Dagh Basin, NE Tethyan realm. *Journal of Iberian Geology*, 44(2): 177–191.
- Kalanat B. and Vaziri-Moghaddam H. 2019a. Ecological changes and depositional sequences during Cenomanian/Turonian platform evolution in the Zagros Basin, SW Iran; an interplay between tectonics and aquifer-eustasy. *Sedimentary Geology*, 390: 31–44.
- Kalanat B. and Vaziri-Moghaddam H. 2019b. The Cenomanian/Turonian boundary interval deep-sea deposits in the Zagros Basin (SW Iran): Bioevents, carbon isotope record and palaeoceanographic model. *Palaeogeography, Palaeoclimatology, Palaeoecology*, 533:109238.
- Kalanat B. Mahmudy Gharai M.H. Vahidinia M. Vaziri-Moghaddam H. Kano A. and Kumon F. 2018b.



- Paleoenvironmental perturbation across the Cenomanian/Turonian boundary of the Kopet-Dagh Basin (NE Iran), inferred from geochemical anomalies and benthic foraminiferal assemblages. *Cretaceous Research*, 86: 261–275.
- Kalanat B. Vahidinia M. Vaziri-Moghaddam H. and Mahmudy Gharaie M.H. 2016. Planktonic foraminiferal turnover across the Cenomanian/Turonian boundary (OAE2) in northeast of Tethys realm, Kopet-Dagh basin. *Geologica Carpathica*, 67: 451–462.
- Kalanat B. Vahidinia M. Vaziri-Moghaddam H. Mahmudy Gharaie M.H. and Kumon F. 2017. Benthic foraminiferal response to environmental changes across Cenomanian/Turonian boundary (OAE2) in the northeastern Tethys, Kopet-Dagh Basin. *Journal of African Earth Science*, 134: 33–47.
- Keller G. 2002. Guembelitria dominated late Maastrichtian planktonic foraminiferal assemblages mimic early Danian in the Eastern Desert of Egypt. *Marine Micropaleontology*, 47 (1-2): 71–99.
- Keller G. Adatte T. Berner Z. Chellai E.H. and Stueben D. 2008. Oceanic events and biotic effects of the Cenomanian–Turonian anoxic event, Tarfaya Basin, Morocco. *Cretaceous Research*, 29: 976–994.
- Keller G. Adatte T. Stinnesbeck W. Luciani V. Karoui N. and Zaghib-Turki D. 2002. Paleocology of the Cretaceous–Tertiary mass extinction in planktonic foraminifera. *Palaeogeography, Palaeoclimatology, Palaeoecology*, 178: 257–298.
- Keller G. and Pardo A. 2004a. Disaster opportunists Guembelitridae: index for environmental catastrophes. *Marine Micropaleontology*, 53: 83–116.
- Keller G. and Pardo A. 2004b. Age and paleoenvironment of the Cenomanian–Turonian global stratotype section and point at Pueblo, Colorado. *Marine Micropaleontology*, 51: 95–128.
- Keller G. Han Q. Adatte T. and Burns S. 2001. Paleoenvironment of the Cenomanian–Turonian transition at Eastbourne, England. *Cretaceous Research*, 22: 391–422.
- Kimoto K. Ishimura T. Tsunogai U. Itaki T. and Ujiie Y. 2009. The living triserial planktonic foraminifer *Gallitellia vivans* (Cushman): Distribution, stable isotopes, and paleoecological implications. *Marine Micropaleontology*, 71: 71–79.
- Kolonis S. Wagner T. Forster A. Sinninghe Damste J.S. Walsworth-Bell B. Erba E. Turgeon, S. Brumsack H.J. Chellai E.H. Tsikos H. Kuhnt W. and Kuypers M.M.M. 2005. Black shale deposition on the northwest African Shelf during the Cenomanian/Turonian oceanic anoxic event: climate coupling and global organic carbon burial. *Paleoceanography*, 20: PA1006.
- Kuhnt W. Herbin J.P. Thurow J. and Wiedmann J. 1990. Distribution of Cenomanian/Turonian organic facies in the western Mediterranean and along the adjacent Atlantic margin, In: Huc A.Y. (Ed.), *Deposition of Organic Facies*. American Association of Petroleum Geologists, Tulsa, Studies in Geology, 133–160.
- Kuhnt W. Holbourn A.E. Beil S. Aquit M. Krawczyk T. Flogel S. Chellai E.H. and Jabour H. 2017. Unraveling the onset of Cretaceous Oceanic Anoxic Event 2 in an extended sediment archive from the Tarfaya-Laayoune Basin, Morocco. *Paleoceanography*, 32: 923–946.
- Kuypers M.M.M. Pancost R.D. and Sinninghe Damsté J.S. 1999. A large and abrupt fall in atmospheric CO₂ concentration during Cretaceous times. *Nature*, 399, 342–345.
- Kuypers M.M.M. Pancost R.D. Nijenhuis I.A. and Sinninghe Damsté J.S. 2002. Enhanced productivity led to increased organic carbon burial in the euxinic North Atlantic basin during the late Cenomanian oceanic anoxic event. *Paleoceanography*, 17(4): PA1051.
- Larson R.L. 1991. Geological consequences of super plumes. *Geology*, 19: 963–966.
- Leckie R.M. Bralower T.J. and Cashman R. 2002. Oceanic anoxic events and plankton evolution: biotic response to tectonic forcing during the mid-Cretaceous. *Paleoceanography*, 17: 13.1–13.29.
- Leckie R.M. Yuretich R.F. West O.L.O. Finkelstein D. and Schmidt M. 1998. Paleocyanography of the southwestern western interior sea during the time of the Cenomanian–Turonian boundary (Late Cretaceous). *Society of Economic Paleontologists and Mineralogists, Concepts in Sedimentology and Paleontology*, 6: 101–126.
- MacLeod K.G. Huber B.T. and Le Ducharme M. 2000. Paleontological and geochemical constraints on the deep ocean during the Cretaceous greenhouse interval, In: Huber B.T. MacLeod K.G. and Wing S.L. (Eds.), *Warm Climates in Earth History*. Cambridge University Press, Cambridge, 241–274.
- Murray J.W. 1991. Ecology and paleoecology of benthic foraminifera. Longman, London, 397 p.
- Muttoni G. Mattei M. Balini M. Zanchi A. Gaetani, M. and Berra F. 2009. The drift history of Iran from the Ordovician to the Triassic. In: Brunet M.-F. Wilmsen M. and Granath J. (Eds.), *South Caspian to Central Iran Basins*. Geological Society of London, Special Publication, 7–29.
- Norris R.D. and Wilson P.A. 1998. Low latitude sea surface temperatures for the mid-Cretaceous and the evolution of planktonic foraminifera. *Geology*, 26: 823–826.
- Pancost R.D. Crawford N. Magness S. Turner A. Jenkyns H.C. and Max-well J.R. 2004. Further evidence for the development of photic-zone euxinic conditions during Mesozoic oceanic anoxic events. *Journal of the Geological Society*, 161: 353–364.
- Pearce M.A. Jarvis I. and Tocher B.A. 2009. The Cenomanian-Turonian boundary event, OAE2 and palaeoenvironmental change in epicontinental seas: new in-sights from the dinocyst and geochemical records. *Palaeogeography, Palaeoclimatology, Palaeoecology*, 280: 207–234
- Pogge von Strandmann P.A.E. Jenkyns H.C. and Woodfine R.G. 2013. Lithium isotope evidence for enhanced weathering during Oceanic Anoxic Event 2. *Nature Geoscience*, 6: 668–672.
- Premoli Silva I. and Sliter W.V. 1999. Cretaceous paleoceanography: evidence from planktonic foraminiferal evolution, In: Barrera E. and Johnson C.C. (Eds.), *Evolution of the Cretaceous ocean-climate system*. Geological Society of America, Special Paper, Boulder, 301–328.
- Premoli Silva I. and Verga D. 2004. Practical manual of Cretaceous planktonic foraminifera, In: Verga D. and Rettori, R. (Eds.), *International School on Planktonic Foraminifera, 3^o Course: Cretaceous*. Universities of Perugia and Milan, Tipografia Pontefelcina, Perugia. 283 p.
- Premoli Silva I. Erba E. Salvini G. Locatelli C. and Verga D. 1999. Biotic changes in Cretaceous Oceanic Anoxic

- Events of the Tethys. *Journal of Foraminiferal Research*, 29: 352–370.
- Price G.D. and Hart M.B. 2002. Isotopic evidence for early to mid-Cretaceous ocean temperature variability. *Marine Micropaleontology*, 46: 45–58.
- Price G.D. Selwood B.W. Corfield R.M. Clarke L. and Cartlidge J.E. 1998. Isotopic evidence for paleotemperatures and depth stratification of Middle Cretaceous planktonic foraminifera from the Pacific Ocean. *Geological Magazine*, 135: 183–191.
- Reolid M. Sánchez-Quiñones C.A. Alegret L. and Molina E. 2015. Palaeoenvironmental turnover across the Cenomanian-Turonian transition in Oued Bahloul, Tunisia: foraminifera and geochemical proxies. *Palaeogeography, Palaeoclimatology, Palaeoecology*, 417: 491–510.
- Robaszynski F. and Caron M. 1995. Foraminifères planctoniques du Crétacé: commentaire de la zonation Europe-Méditerranée. *Bull. Soc. Géol. France*, 166: 681–692.
- Robert A. Letouzey J. Kavooosi M.A. Sherhati S. Müller C. Vergés J. and Aghababaei A. 2014. Structural evolution of the Kopeh Dagh fold-and-thrust belt (NE Iran) and interactions with the South Caspian Sea Basin and Amu Darya Basin. *Marine and Petroleum Geology*, 57: 68–87.
- Schlanger S.O. and Jenkyns H.C. 1976. Cretaceous oceanic anoxic events: Causes and consequences. *Geologie en Mijnbouw*, 55: 179–184.
- Schlanger S.O. Arthur M.A. Jenkyns H.C. and Scholle P.A. 1987. The Cenomanian–Turonian oceanic anoxic event, I. Stratigraphy and distribution of organic carbon-rich beds and the marine ¹³C excursion, In: Brooks J. and Fleet J.A. (Eds.), *Marine Petroleum Source Rocks*. Geological Society, Special Publications, 26, London, 371–399.
- Scholle P.A. and Arthur M.A. 1980. Carbon isotope fluctuations in Cretaceous pelagic limestones: potential stratigraphic and petroleum exploration tool. *American Association of Petroleum Geologists Bulletin*, 64: 67–87.
- Seton M. Gaina C. Muller R.D. and Heine C. 2009. Mid-Cretaceous sea floor spreading pulse: fact or fiction? *Geology*, 37: 687–690.
- Snow L.J. Duncan R.A. and Bralower T.J. 2005. Trace element abundances in the Rock Canyon Anticline, Pueblo, Colorado, marine sedimentary section and their relationship to Caribbean plateau construction and oxygen anoxic event 2. *Paleoceanography*, 20: P A3005.
- Spero H.J. Bijma J. Lea D.W. and Bemis B.E. 1997. Effect of seawater carbonate concentration on foraminiferal carbon and oxygen isotopes. *Nature*, 390: 497–500.
- Stampfli G.M. and Borel G.D. 2002. A plate tectonic model for the Paleozoic and Mesozoic constrained by dynamic plate boundaries and restored synthetic oceanic isochrones. *Earth and Planetary Science Letters*, 196: 17–33.
- Turgeon S.C. and Creaser R.A. 2008. Cretaceous oceanic anoxic event 2 triggered by a massive magmatic episode. *Nature*, 454: 323–326.
- Voigt S. Gale A.S. and Fogel S. 2004. Mid latitude shelf seas in the Cenomanian-Turonian greenhouse world: temperature evolution and North Atlantic circulation. *Paleoceanography*, 19: PA4020.
- Wendler I. Huber B.T. MacLeod K.G. and Wendler, J.E., 2013. Stable oxygen and carbon isotope systematics of exquisitely preserved Turonian foraminifera from Tanzania-Understanding isotopic signatures in fossils. *Marine Micropaleontology*, 102: 1–33.
- Wendler I. Wendler J.E. and Clarke L.J. 2016a. Sea-level reconstruction for Turonian sediments from Tanzania based on integration of sedimentology, microfacies, geochemistry and micropaleontology. *Palaeogeography, Palaeoclimatology, Palaeoecology*, 441 (3): 528–564.
- Wendler J.E. Meyers S.R. Wendler I. Vogt C. and Kuss J. 2011. Drivers of cyclic sea-level changes during the Cretaceous green-house: A new perspective from the Levant Platform. Geological Society of London, Special Publication, 43: 376.
- Wendler J.E. Wendler I. Vogt C. and Kuss J. 2016b. Link between cyclic eustatic sea-level change and continental weathering: Evidence for aquifer-eustasy in the Cretaceous. *Palaeogeography, Palaeoclimatology, Palaeoecology*, 441: 430–437.
- West O.L.O. Leckie R.M. and Schmidt M. 1998. Foraminiferal paleoecology and paleoceanography of the Greenhorn Cycle along the southwestern margin of the Western Interior Sea. *SEPM Concepts Sedimentology Paleontology*, 6: 79–99.
- Zaric S. Donner B. Fischer G. Mulitza S. and Wefer G. 2005. Sensitivity of planktonic foraminifera to sea surface temperature and export production as derived from sediment trap data. *Marine Micropaleontology*, 55: 75–105.

Supplementary Table 1- planktonic foraminifera in the Shurab section.

| Biozone | <i>R. cushmani</i> | | | | | | | | | | | <i>W. arch.</i> | | |
|--|--------------------|-----|------|------|-----|-----|-----|-----|-----|-----|-----|-----------------|-----|-----|
| Sample number | 42 | 46 | 50 | 54 | 58 | 62 | 66 | 70 | 74 | 78 | 84 | 88 | 90 | 92 |
| <i>Clavhedbergella. simplex</i> | | | | | | | | | 2 | 1 | 6 | 1 | 5 | 4 |
| <i>Dicarinella elata</i> | | | | | | | | | | | | 1 | | |
| <i>D. hagni</i> | | | | | 2 | | | 4 | | 5 | 5 | 44 | | |
| <i>D. imbricata</i> | | | | | | | | 1 | | 3 | | 2 | | |
| <i>Guembelitra cenomana</i> | 26 | 44 | 43 | 35 | 50 | 55 | 18 | 42 | 35 | 12 | 24 | 21 | 32 | 39 |
| " <i>Globigerinelloides</i> " <i>bentonensis</i> | 15 | 5 | 1 | | | 3 | 1 | | 1 | | | | | |
| <i>G. ultramicrus</i> | 19 | 7 | 13 | 5 | 8 | 3 | 6 | | 11 | 33 | 61 | 44 | 3 | 4 |
| <i>Helvetoglobotruncana helvetica</i> | | | | | | | | | | | | | | |
| <i>H. praehelvetica</i> | | | | | | | | | | | | | | |
| <i>Laeviheterohelix pulcra</i> | 14 | 4 | 1 | | 2 | 1 | | 3 | | 4 | | | | |
| <i>Loeblichella hessi</i> | | | | | 1 | | | | 6 | | | | | |
| <i>Muricohedbergella delrioensis</i> | 7 | 10 | 11 | 3 | 7 | 6 | | 9 | 18 | 13 | 7 | 8 | | 13 |
| <i>M. planispira</i> | 5 | | | | | | | | | | | | | 1 |
| <i>Planoheterohelix globulosa</i> | 1 | | | 3 | | | | 1 | | | | | | |
| <i>P. moremani</i> | 14 | 8 | 1 | 4 | 8 | 4 | | | | 1 | 11 | 19 | 3 | 6 |
| <i>P. reussi</i> | 19 | 54 | 6 | 33 | 41 | 38 | 5 | 12 | 16 | 77 | 48 | 38 | 77 | 50 |
| <i>Praeglobotruncana algeriana</i> | 1 | 1 | | | 12 | 2 | | 9 | | 10 | 2 | | | |
| <i>P. delrioensis</i> | 3 | | | | 16 | 1 | 12 | 2 | | 6 | 6 | | 1 | |
| <i>P. gibba</i> | | | | | 1 | | | 2 | | 6 | 3 | | 4 | |
| <i>P. stephani</i> | | | | | 3 | | | | | 13 | 1 | | 2 | 1 |
| <i>p. hilalensis</i> | | | | | | | | | | | | | 1 | |
| <i>Rotalipora cushmani</i> | 4 | | | | 1 | 1 | | 2 | 2 | 1 | 6 | | | |
| <i>R. montsalvensis</i> | | | | | | | | 1 | | | | | | |
| <i>Thalmaninella appenninica</i> | 12 | | | 2 | | | | 3 | | | 1 | | | |
| <i>T. brotzeni</i> | | | | | | | | | | 3 | | | | |
| <i>Whiteinella aprica</i> | 16 | 18 | 15 | 9 | 21 | 17 | 27 | 29 | 36 | 23 | 19 | 23 | 18 | 25 |
| <i>W. aumalensis</i> | | | | | | | | | | | | | 1 | |
| <i>W. archaeocretacea</i> | 13 | 10 | 8 | | 5 | 7 | 3 | 30 | 15 | 5 | 5 | 24 | 10 | 14 |
| <i>W. baltica</i> | 133 | 140 | 203 | 202 | 118 | 161 | 129 | 158 | 159 | 88 | 96 | 91 | 141 | 144 |
| <i>W. brittonensis</i> | | | | | 2 | 1 | | 1 | 1 | | | 5 | 7 | 2 |
| <i>W. paradubia</i> | | | | | | | | | | | | 1 | 8 | |
| Species richness | 15 | 11 | 10 | 9 | 18 | 14 | 7 | 17 | 12 | 18 | 17 | 17 | 13 | 12 |
| Total species counted | 301 | 301 | 302 | 296 | 398 | 299 | 201 | 309 | 302 | 304 | 301 | 328 | 313 | 303 |
| H(s) | 2 | 1.6 | 1.18 | 1.11 | 1.8 | 1.4 | 1.2 | 1.7 | 1.6 | 2.1 | 2 | 2.1 | 1.5 | 1.6 |

Supplementary Table 1 (continued)

| Biozone | <i>W. archaeocretacea</i> | | | | | | | | | | | | <i>H. h.</i> | |
|--|---------------------------|-----|-----|-----|-----|-----|-----|-----|-----|-----|-----|-----|--------------|-----|
| Sample number | 94 | 96 | 98 | 105 | 109 | 113 | 117 | 119 | 121 | 125 | 129 | 133 | 136 | 139 |
| <i>Clavhedbergella simplex</i> | 2 | 12 | 8 | | | | | | | | | | | |
| <i>Dicarinella elata</i> | | | | | | | | | | | | | | |
| <i>D. hagni</i> | 1 | | 6 | | | | | 9 | | 5 | 2 | 2 | 3 | 7 |
| <i>D. imbricata</i> | | | | | | | | | | | | | 2 | 2 |
| <i>Guembelitra cenomana</i> | 22 | 6 | 10 | 20 | 5 | 7 | 7 | 8 | 5 | 4 | 1 | 5 | | 2 |
| " <i>Globigerinelloides</i> " <i>bentonensis</i> | | | | | | | | | | | | | | |
| <i>G. ultramicrus</i> | | | | | | | | | | | | 6 | 5 | 3 |
| <i>Helvetoglobotruncana helvetica</i> | | | | | | | | | | | | | 1 | 1 |
| <i>H. praehelvetica</i> | | | | 1 | 1 | | | | | 3 | | | | |
| <i>Laeviheterohelix pulcra</i> | | 1 | 6 | 3 | 1 | 6 | 6 | | | | | 1 | | |
| <i>Loeblichella hessi</i> | 3 | 2 | 1 | 23 | 7 | 7 | 7 | 9 | 6 | 7 | 2 | 2 | 2 | 2 |
| <i>Muricohedbergella delrioensis</i> | 3 | 5 | 4 | 11 | 5 | 3 | 3 | 8 | 8 | 2 | | 6 | 1 | 1 |
| <i>M. planispira</i> | | | | | | | | | | | | | | |
| <i>Planoheterohelix globulosa</i> | | | | | | | | | | | | | | |
| <i>P. moremani</i> | 12 | 14 | 14 | 18 | 18 | 22 | 22 | 15 | 14 | 11 | 7 | 14 | 17 | 4 |
| <i>P. reussi</i> | 63 | 65 | 62 | 72 | 100 | 95 | 95 | 92 | 105 | 108 | 116 | 95 | 95 | 100 |
| <i>Praeglobotruncana algeriana</i> | | | | 1 | 2 | 3 | 3 | 3 | | 2 | | | | 4 |
| <i>P. delrioensis</i> | 2 | | 3 | | | | | | | 5 | | | 2 | 4 |
| <i>P. gibba</i> | 1 | | 1 | | | | | | | | | 1 | | |
| <i>p. hilalensis</i> | | | | | | | | | | | | | | |
| <i>P. stephani</i> | | | 2 | | | | | 2 | | 4 | 3 | | 3 | |
| <i>Rotalipora cushmani</i> | | | | | | | | | | | | | | |
| <i>R. montsalvensis</i> | | | | | | | | | | | | | | |
| <i>Thalmaninella appenninica</i> | | | | | | | | | | | | | | |
| <i>T. brotzeni</i> | | | | | | | | | | | | | | |
| <i>Whiteinella aprica</i> | 15 | 25 | 38 | 25 | 41 | 14 | 14 | 23 | 30 | 16 | 43 | 38 | 28 | 20 |
| <i>W. aumalensis</i> | | | 1 | 2 | 1 | | | | | | | | | |
| <i>W. archaeocretacea</i> | 14 | 4 | 15 | 10 | 24 | 9 | 9 | | 10 | 10 | 8 | 19 | 11 | 14 |
| <i>W. baltica</i> | 111 | 142 | 131 | 114 | 87 | 125 | 140 | 132 | 123 | 96 | 112 | 128 | 121 | 144 |
| <i>W. brittonensis</i> | 1 | 18 | 1 | 1 | 2 | 2 | 2 | 3 | 1 | | 3 | 1 | 4 | 1 |
| <i>W. inornata</i> | | | | | | 1 | 1 | | | | | | | |
| <i>W. paradubia</i> | 3 | 5 | 5 | 5 | 4 | 1 | 1 | 3 | 2 | 4 | 2 | 5 | 6 | 2 |
| Species richness | 14 | 12 | 17 | 14 | 14 | 13 | 13 | 12 | 10 | 14 | 11 | 14 | 15 | 16 |
| Total species counted | 238 | 299 | 308 | 306 | 298 | 293 | 310 | 307 | 304 | 277 | 299 | 323 | 301 | 291 |
| H(s) | 1.7 | 1.6 | 1.8 | 1.8 | 1.7 | 1.6 | 1.5 | 1.6 | 1.5 | 1.6 | 1.4 | 1.6 | 1.6 | 1.5 |

